Development 135, 1513-1524 (2008) doi:10.1242/dev.014340

Polycomb group proteins Ring1A/B are functionally linked to the core transcriptional regulatory circuitry to maintain ES cell identity

Mitsuhiro Endoh[1], Takaho A. Endo[2], Tamie Endoh[1], Yu-ichi Fujimura[1], Osamu Ohara[1], Tetsuro Toyoda[2], Arie P. Otte[3], Masaki Okano[4], Neil Brockdorff[5], Miguel Vidal[1,6] and Haruhiko Koseki[1,*]

The Polycomb group (PcG) proteins mediate heritable silencing of developmental regulators in metazoans, participating in one of two distinct multimeric protein complexes, the Polycomb repressive complexes 1 (PRC1) and 2 (PRC2). Although PRC2 has been shown to share target genes with the core transcription network, including Oct3/4, to maintain embryonic stem (ES) cells, it is still unclear whether PcG proteins and the core transcription network are functionally linked. Here, we identify an essential role for the core PRC1 components Ring1A/B in repressing developmental regulators in mouse ES cells and, thereby, in maintaining ES cell identity. A significant proportion of the PRC1 target genes are also repressed by Oct3/4. We demonstrate that engagement of PRC1 at target genes is Oct3/4-dependent, whereas engagement of Oct3/4 is PRC1-independent. Moreover, upon differentiation induced by Gata6 expression, most of the Ring1A/B target genes are derepressed and the binding of Ring1A/B to their target loci is also decreased. Collectively, these results indicate that Ring1A/B-mediated Polycomb silencing functions downstream of the core transcriptional regulatory circuitry to maintain ES cell identity.

KEY WORDS: Polycomb, Oct3/4 (Pou5f1), Gata6, ES cells, Chromatin, Silencing, Ring1A/B (Ring1/Rnf2), Mouse

INTRODUCTION

Embryonic stem (ES) cells derived from the inner cell mass (ICM) of mammalian blastocyst-stage embryos have unlimited growth potential while maintaining pluripotency – the ability to differentiate into all tissue types except the placenta (Evans and Kaufman, 1981; Martin, 1981). These properties of ES cells are maintained by symmetrical self-renewal, producing two identical stem cell daughters upon cell division (Burdon et al., 2002). The maintenance of ES cell pluripotency is thought to involve a transcriptional regulatory hierarchy including the transcription factors Oct3/4 (Pou5f1 – Mouse Genome Informatics), Sox2 and Nanog, which may be central components judging by their unique expression patterns and essential roles during early murine development (Avilion et al., 2003; Chambers et al., 2003; Mitsui et al., 2003; Nichols et al., 1998).

Recent genome-wide chromatin immunoprecipitation (ChIP) analyses revealed that OCT4, SOX2 and NANOG co-occupy the promoters of a large group of genes in human ES cells (Boyer et al., 2005), suggesting that these factors form a core regulatory feedback circuit, in which all three factors regulate the expression of themselves as well as of each other (Catena et al., 2004; Kuroda et al., 2005; Okumura-Nakanishi et al., 2005; Rodda et al., 2005). This positive-feedback loop promotes self-renewal of pluripotent ES cells by repressing transcription factors involved in differentiation and development, whilst likely activating the expression of genes involved in ES cell maintenance (Boyer et al., 2005).

The execution of differentiation programs in ES cells is likely to be preceded by interruption of the positive-feedback loop by developmental regulators such as Cdx2 and Gata6. The expression of Cdx2 and Gata6 is repressed by Oct3/4 and Nanog in undifferentiated ES cells (Boyer et al., 2005; Loh et al., 2006; Mitsui et al., 2003; Niwa et al., 2000; Niwa et al., 2005), and the enforced expression of Cdx2 and Gata6 quickly shuts down the positive loop and promotes a rapid transition from the undifferentiated to the differentiated state (Fujikura et al., 2002; Niwa et al., 2005). Therefore, the positive-feedback loops and developmental regulators are reciprocally engaged to maintain ES cell identity; however, the molecular mechanisms underlying this reciprocal interaction are not fully understood.

The Polycomb group (PcG) of proteins mediate heritable silencing of developmental regulators in metazoans, participating in one of two distinct multimeric protein complexes, the Polycomb repressive complexes 1 (PRC1) and 2 (PRC2) (Cao et al., 2002; Czermin et al., 2002; Kuzmichev et al., 2002; Muller et al., 2002; Shao et al., 1999). In mammals, the core PRC2 is composed of Eed, Ezh2 and Suz12 and catalyses trimethylation of histone H3 at lysine 27 (H3K27), which in turn is thought to provide a recruitment site for PRC1 (Cao et al., 2002; Czermin et al., 2002; Fischle et al., 2003; Kuzmichev et al., 2002; Min et al., 2003). The core PRC1 is composed of orthologs of *Drosophila* Polycomb (Cbx2, Cbx4 and Cbx8), Posterior sex combs [Mel18 (Pcgf2) and Bmi1], Sex comb extra (Ring1A and Ring1B, also known as Ring1 and Rnf2, respectively – Mouse Genome Informatics) and Polyhomeotic (Phc1, Phc2 and Phc3). Recent studies demonstrate that mono-ubiquitylation of histone H2A at lysine 119 is important in PcG-mediated silencing, with Ring1A/B functioning as the E3 ligase in this reaction (de Napoles et al., 2004; Wang et al., 2004).

[1]RIKEN Research Center for Allergy and Immunology, and [2]RIKEN Genomic Sciences Center, 1-7-22 Suehiro, Tsurumi-ku, Yokohama 230-0045, Japan. [3]Swammerdam Institute for Life Sciences, University of Amsterdam, Kruislaan 406, 1098 SM Amsterdam, The Netherlands. [4]RIKEN Center for Developmental Biology, 2-2-3 Minatojima-minamimachi, Chuo-ku, Kobe, Hyogo 6500047, Japan. [5]Developmental Epigenetics Group, MRC Clinical Sciences Centre, ICFM, Hammersmith Hospital, DuCane Road, London W12 ONN, UK. [6]Centro de Investigaciones Biologicas, Department of Developmental and Cell Biology, Ramiro de Maeztu 9, 28040 Madrid, Spain.

*Author for correspondence (e-mail: koseki@rcai.riken.jp)

Accepted 29 January 2008

Mouse and human ES cells have recently been analyzed by genome-wide ChIP, and PRC1 and PRC2 have been shown to repress genes involved in processes including development, transcriptional regulation and morphogenesis, via direct interactions with target genes (Boyer et al., 2006; Lee et al., 2006). Notably, PRC2 has been shown to share target genes with OCT4, SOX2 and/or NANOG in human ES cells (Lee et al., 2006). However, it is still unclear whether PcG and the core transcription network are functionally linked to regulate expression of their target genes.

In this study, we addressed the role of PRC1 in mouse ES cell maintenance and its functional interaction with the core transcriptional regulatory circuitry. We find that PRC1 is essential for the maintenance of ES cell identity and for the repression of developmental regulators by inhibiting chromatin remodeling. We go on to show that Ring1A/B-mediated PcG silencing is Oct3/4-dependent, whereas it is abolished by developmental cues resulting in *Gata6* activation. Collectively, our data suggest that Ring1A/B-mediated Polycomb silencing functions downstream of the core transcriptional regulatory circuitry to maintain ES cell self-renewal.

MATERIALS AND METHODS

Mouse cells

Eed-KO, *Dnmt1*-KO, *Oct3/4* conditional KO (ZHBTc4) ES cell lines and the ES cell line expressing a Gata6-GR fusion (G6GR) were described previously (Azuara et al., 2006; Lei et al., 1996; Niwa et al., 2000; Shimosato et al., 2007). Generation of mutant *Ring1A* and *Ring1B* flox alleles were described previously (Cales et al., 2008; del Mar Lorente et al., 2000). *Rosa26*::*CreERT2* transgenic mice were purchased from Artemis Pharmaceuticals (Seibler et al., 2003). *Ring1A*$^{-/-}$;*Ring1B*$^{fl/fl}$;*Rosa26*::*CreERT2* ES cells were derived from blastocysts. Male ES cells were used in this study.

Immunoprecipitation (IP) and chromatin immunoprecipitation (ChIP) analyses

IP (Isono et al., 2005a) and ChIP (Orlando et al., 1997) were performed as previously described. Immunoprecipitated and input DNA were quantified by real-time PCR. Primer and probe sequences are available upon request. Antibodies used in this study are listed in Table 1.

Reverse transcription and quantitative real-time PCR

RNA extraction and cDNA synthesis were performed as described previously (Isono et al., 2005b). Quantitative real-time PCR was carried out using the SYBR Green (Stratagene, Agilent Technologies, Santa Clara, CA) or Taqman (Biosearch Technologies, Novato, CA) method and amplifications detected with an Mx3005P (Stratagene, La Jolla, CA). Primer and probe sequences are available upon request.

Microarray methods and data analysis

Total RNA was extracted using Trizol (Invitrogen, Carlsbad, CA) and purified with RNeasy separation columns (Qiagen, Hilden, Germany). First-strand cDNA was synthesized and hybridized to Affymetrix GeneChip Mouse Genome 430 2.0 arrays (Affymetrix, Santa Clara, CA) to assess and compare the overall gene expression profiles.

To obtain normalized intensities from at least two slides, the quantile normalization method was used for every feature on the array (Bolstad et al., 2003). We calculated the log of the ratio of intensity in the knockout (KO) samples to the intensity in the respective control samples. Probes were not applied for further analysis when signals were at insignificant levels in control and KO samples. The expression change of a gene was calculated using the geometric mean of all probes aligned on the gene.

The microarray and ChIP-chip data are available in the NCBI Gene Expression Omnibus (GEO) under the series GSE10573 [NCBI GEO] with sample accession numbers GSM265040 to GSM265045, GSM266065 to GSM266067, GSM266076, GSM266077, GSM266115, GSM266837 and GSM266838.

Comparable expression analyses between KO ES cells

We obtained Pearson product-moment correlation coefficients of the logarithms of expression changes between respective KO ES cells. The 95% confidence intervals of correlation coefficients were calculated using Z transformation. Eigenvalues and eigenvectors of the distribution in scatter diagrams were calculated using principal component analysis with software R (http://www.r-project.org/).

Gene ontology (GO) analysis

We performed GO analysis using our in-house programs written in Python and C++ and GO data retrieved from the Gene Ontology database (http://www.geneontology.org), KEGG (http://www.genome.jp/kegg/) and others (Auernhammer and Melmed, 2000; Heinrich et al., 2003). The version of the dataset used was Oct 27th, 2006, submitted by Mouse Genome Informatics (MGI). We aligned microarray probes on mouse genes and assigned GO terms on all probes using these alignments. The significance of each GO term was determined using Fisher's exact test and Bonferroni adjustment for multiple testing. The *P*-value reflects the likelihood that we would observe such enrichment or higher by chance. Subsequent statistical examinations were also conducted using Fisher's exact test.

ChIP-chip experiment, assignment of IP regions and calculation of fold enrichment

ChIP-on-chip analysis of Ring1B binding was carried out using the Mouse Promoter ChIP-on-chip Microarray Set (G4490A; Agilent Technologies). ES cells were subjected to ChIP assay using anti-Ring1B antibody as described (Fujimura et al., 2006). Purified immunoprecipitated and input DNA were subjected to blunt ligation with linker oligo DNA, linker-

Table 1. Antibodies used in this study

Target protein	Species and clonality	Experiment	Source/reference
Oct3/4	Mouse monoclonal (C-10)	WB, IP	Santa Cruz (sc-5279)
Oct3/4	Goat polyclonal	ChIP	Santa Cruz (sc-8628X)
Ring1B	Mouse monoclonal (#3)	WB, IP, ChIP	(Atsuta et al., 2001)
Phc1	Mouse monoclonal	WB, ChIP	(Miyagishima et al., 2003)
Mel18	Goat polyclonal	WB	Abcam (ab5267)
Cbx2	Mouse monoclonal (2C6)	WB	(Fujimura et al., 2006)
Rybp	Rabbit polyclonal	WB	(Garcia et al., 1999)
Eed	Mouse monoclonal (M26)	WB, ChIP	(Hamer et al., 2002)
Suz12	Mouse monoclonal (4F7)	WB	Made in our laboratory
Ezh2	Mouse monoclonal (M10)	WB	(Hamer et al., 2002)
Acetylated histone H3	Rabbit polyclonal	WB, ChIP	Millipore/Upstate (06-599)
Trimethylated histone H3-K4	Rabbit polyclonal	WB, ChIP	Millipore/Upstate (07-473)
Trimethylated histone H3-K27	Rabbit polyclonal	WB, ChIP	Millipore/Upstate (07-449)
Ubiquitylated histone H2A	Mouse monoclonal (E6C5)	WB	Millipore/Upstate (05-678)
RNA polymerase II	Mouse monoclonal (8WG16)	ChIP	Millipore/Upstate (05-952)
Lamin B	Goat polyclonal	WB	Santa Cruz (sc-6216)

WB, western blot; IP, immunoprecipitation; ChIP, chromatin immunoprecipitation.

mediated PCR (LM-PCR), labeling, hybridization and washing following the Agilent mammalian ChIP-on-chip protocol. Scanned images were quantified with Agilent Feature Extraction software under standard conditions.

Assignment of regions bound by Ring1B around transcription start sites (TSSs) was carried out using direct sequence alignment on the mouse genome database (NCBI version 36). The location of Ring1B-bound regions was compared with a set of transcripts derived from the MGI database. We assigned bound regions that were within –8 kb to +2 kb of the TSS. Alignments on mouse genome and TSSs of genes were retrieved from Ensembl (http://www.ensembl.org).

The measured intensity ratios (IP/input: fold enrichment) were calculated, and the maximum value of the ratios in each promoter region (–8 kb to +2 kb around TSS) of a gene was used to represent the fold enrichment of the gene. Fold enrichment was calculated only for probes whose signals both from IP and input DNAs were significant ($P<10^{-3}$).

RESULTS

Ring1A/B are required for the maintenance of ES cell identity

To investigate the role of PRC1 for maintenance of mouse ES cell identity, it was necessary to generate *Ring1A/B* double-knockout (dKO) ES cells because *Ring1B* single-knockout (*Ring1B*-KO) ES cells can be cultured for >20 passages and exhibit ES cell morphology (de Napoles et al., 2004; Fujimura et al., 2006) (data not shown). Thus, we established *Ring1A*$^{-/-}$;*Ring1B*$^{fl/fl}$;*Rosa26*::*CreERT2* ES cell lines, in which *Ring1B* could be conditionally deleted by 4-hydroxy tamoxifen (OHT) treatment. Ring1B protein levels were dramatically depleted within 48 hours of OHT administration (Fig. 1A), and loss of Ring1B resulted in reduced levels of other PRC1 components Mel18, Phc1/2 and Cbx2 (Fujimura et al., 2006; Leeb and Wutz, 2007). At a global level, PRC1-regulated mono-ubiquitylated histone H2A (H2Aub1) was rapidly depleted within 48 hours following OHT treatment (Fig. 1B). We thus concluded that PRC1 could be conditionally depleted in this ES cell line by OHT.

In the *Ring1A/B*-dKO, in contrast to the *Ring1B*-KO ES cells, proliferation was halted and the cells gradually lost typical ES cell morphology after OHT administration (Fig. 1C). Moreover, genome-wide mRNA analysis revealed preferential derepression of genes involved in differentiation and/or developmental processes (Fig. 1D; see also Table S1 in the supplementary material). These observations, considered together with structural and biochemical similarities of Ring1A and Ring1B (Buchwald et al., 2006), led us to hypothesize a compensatory role of Ring1A for Ring1B in the repression of developmental genes in ES cells. This idea is partly supported by the increased expression of Ring1A protein observed in the *Ring1B*-KO ES cells (see Fig. S1 in the supplementary material). We first compared gene expression between the *Ring1A/B*-dKO and *Ring1B*-KO ES cells by microarray analyses. We found that 491 genes were derepressed more than 2-fold in *Ring1B*-KO (constitutive), whereas in *Ring1A/B*-dKO (day 4) ES cells, 999 genes were derepressed (see Table S2 in the supplementary material). Fold expression changes for respective probes in *Ring1A/B*-dKO and *Ring1B*-KO ES cells, determined against the parental or wild-type cells, were plotted on a scatter diagram and the correlation was calculated according to Pearson (see Fig. S2 in the supplementary material). We found a strong correlation (r=0.386) in total calculable genes (see Fig. S2 in the supplementary material). This result indicates significant overlap of genes derepressed in *Ring1A/B*-dKO and *Ring1B*-KO ES cells. The level of derepression was much higher in *Ring1A/B*-dKO than in *Ring1B*-KO ES cells, as represented by differences in variance (see Fig. S2 in the supplementary material). On average, developmental genes were 1.389-fold derepressed in *Ring1A/B*-dKO ES cells, but 1.046-fold in *Ring1B*-KO (see Table S3 in the supplementary material). We confirmed these quantitative differences by evaluating the expression levels of several developmental regulators including *Gata6* and *Cdx2* by quantitative RT-PCR. These genes were significantly derepressed by conditional depletion of Ring1B, but the degree of derepression was higher in the *Ring1A/B*-dKO than in the *Ring1B*-KO cells (Fig. 1E). Therefore, Ring1A and Ring1B appear to act in a compensatory manner to repress the expression of developmental regulators in ES cells and consequently contribute to the maintenance of ES cells in an undifferentiated state. The phenotypic differences between *Ring1B*-KO and *Ring1A/B*-dKO ES cells are likely to be due to exaggerated derepression of developmental regulators such as *Gata6* and *Cdx2* in the dKO cells.

We next examined whether the derepression of developmental regulators is accompanied by disruption of the core transcriptional regulatory circuitry in ES cells. We performed multicolor immunofluorescence analysis for Oct3/4 and for Gata4, which is also expressed in primitive endoderm. Oct3/4 was expressed relatively uniformly in all of the control cells and Gata4 was also expressed in most of the cells (Fig. 1F, upper panels). Four days after OHT administration, we found striking heterogeneity in Oct3/4 expression (Fig. 1F, lower panels). In the example illustrated, most of the cells are compacted; however, a subset of cells at the edge spread out from the colony and exhibit epithelial cell morphology. Most of these cells expressed Gata4 but not Oct3/4 (Fig. 1F, arrowheads in lower right panel), which is likely to be indicative of the onset of spontaneous differentiation. Taken together with the gene expression analysis, these results indicate that Ring1A/B contribute crucially to the repression of ES cell differentiation and therefore to the maintenance of ES cell identity.

Ring1A/B mediate repression of developmental regulators by inhibiting chromatin remodeling via direct binding

We next used ChIP analysis to determine whether genes derepressed in *Ring1A/B*-dKO ES cells were direct targets of PRC1. As shown in Fig. 2A, we observed binding of Ring1B and Phc1, another component of PRC1, to *Hoxb8*, *Gata6*, *Cdx2*, *Zic1* and *T*, all of which are derepressed in the *Ring1A/B*-dKO (Fig. 1E). Binding to all these genes was significantly reduced 2 days after administration of OHT in *Ring1A*$^{-/-}$;*Ring1B*$^{fl/fl}$;*Rosa26*::*CreERT2* ES cells, suggesting that Ring1B is essential for the establishment of PRC1 at their respective loci.

We next examined whether genes derepressed in *Ring1A/B*-dKO ES cells were bound by Ring1B at their promoters using a ChIP-chip approach (Fig. 2B; see Tables S4 and S5 in the supplementary material). We identified almost the same set of Ring1B targets that had been reported previously, if a certain threshold is adopted to distinguish genes bound by Ring1B (Boyer et al., 2006) (data not shown). We further clarified linear correlations between the degree of Ring1B binding and derepression in *Ring1B*-KO and *Ring1A/B*-dKO ES cells (Fig. 2B). These results indicate that Ring1A/B generally repress transcription by directly binding to the target loci in a dose-dependent manner.

Recent studies have demonstrated that PcG targets in ES cells are often characterized by a unique chromatin configuration, being simultaneously enriched for histone modifications associated with gene activity [histone H3 lysine 4 trimethylation (H3K4me3) and lysine 9/14 acetylation (H3Ac)] and modifications associated with PcG-mediated repression [specifically H3K27 trimethylation

(H3K27me3)] (Azuara et al., 2006; Bernstein et al., 2006). With this in mind, we investigated changes in chromatin configuration upon Ring1A/B depletion. At a global level, PRC1-mediated H2Aub1 was rapidly depleted (Fig. 1B). By contrast, there was no detectable change in overall levels of either H3K4me3, H3Ac, H3K27me3 or PRC2 components (see Fig. S3 in the supplementary material). We then analyzed promoter regions of selected PcG target loci derepressed in *Ring1A/B*-dKO ES cells by ChIP. In addition to histone modifications, we analyzed binding of Eed and non-phosphorylated RNA polymerase II (RNAPII) (Fig. 2C). Levels of H3Ac, H3K4me3 and RNAPII binding were significantly increased, whereas those of Eed and H3K27me3 were decreased. Although the molecular mechanism for the decrease in Eed binding upon Ring1A/B depletion is unclear, it is possible that changes in chromatin structure caused by Ring1A/B depletion might secondarily affect Eed binding.

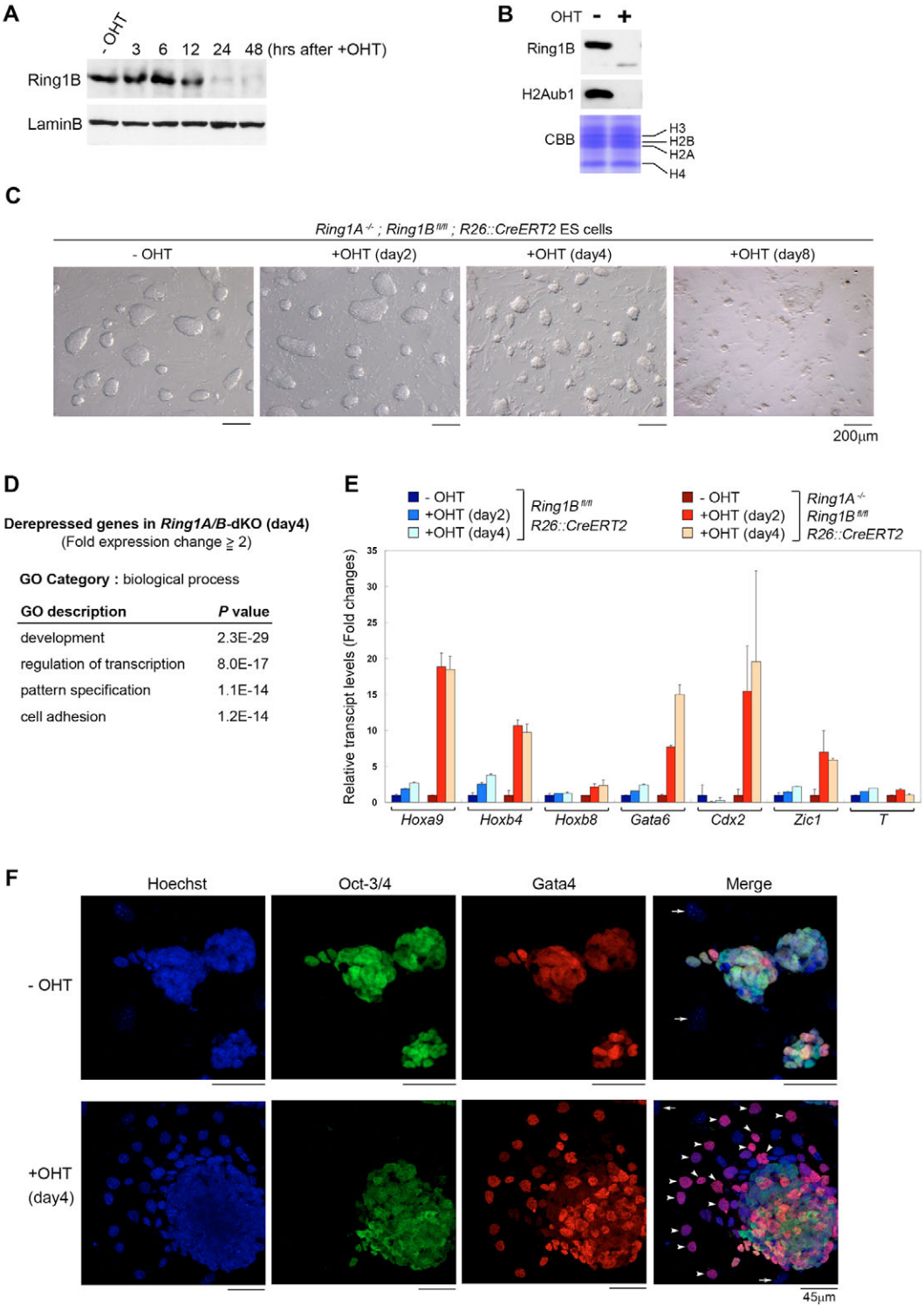

Fig. 1. See next page for legend.

Fig. 1. Ring1A/B are required for the maintenance of mouse ES cell identity. (**A**) Western blot analysis showing the kinetics of Ring1B depletion at 0, 3, 6, 12, 24 and 48 hours after treatment of *Ring1A*$^{-/-}$;*Ring1B*$^{fl/fl}$;*Rosa26*::*CreERT2* ES cells with 4-hydroxy tamoxifen (OHT). Lamin B served as a loading control. (**B**) Western blot showing Ring1B and mono-ubiquitylated H2A (H2Aub1) depletion 2 days after treatment with OHT in *Ring1A*$^{-/-}$;*Ring1B*$^{fl/fl}$;*Rosa26*::*CreERT2* ES cells. OHT was present in (+) or absent from (–) the ES cell culture medium. Coomassie Brilliant Blue (CBB) staining for histones was used as a loading control. (**C**) Morphology of conditional *Ring1A/B*-dKO ES cells. *Ring1A*$^{-/-}$;*Ring1B*$^{fl/fl}$;*Rosa26*::*CreERT2* ES cells were cultured in the absence (–OHT) or presence (+OHT) of OHT, which represent the single *Ring1A*-KO or *Ring1A/B*-dKO cells, respectively. At day 2, *Ring1A/B*-dKO ES cells retain ES-cell-like morphology; however, from day 3-4, *Ring1A/B*-dKO ES cells begin to lose ES-cell-like morphology. (**D**) Gene ontology (GO) analysis of genes more than 2-fold derepressed 4 days after OHT treatment of *Ring1A*$^{-/-}$;*Ring1B*$^{fl/fl}$;*Rosa26*::*CreERT2* ES cells. The significance (*P*-value) of the enrichment of each GO term is indicated for each category of biological process. For details, see Table S1 in the supplementary material. (**E**) Changes in expression levels of *Hoxa9*, *Hoxb4*, *Hoxb8*, *Gata6*, *Cdx2*, *Zic1* and *T* at 2 and 4 days after OHT treatment (+OHT) of *Ring1B*$^{fl/fl}$;*Rosa26*::*CreERT2* or *Ring1A*$^{-/-}$;*Ring1B*$^{fl/fl}$;*Rosa26*::*CreERT2* ES cells as determined by real-time PCR. Expression levels were normalized to an *Actb* control and are depicted as fold changes relative to the OHT-untreated (–OHT) ES cells. Error bars are based on the s.d. as derived from triplicate PCR reactions. (**F**) *Ring1A*$^{-/-}$;*Ring1B*$^{fl/fl}$;*Rosa26*::*CreERT2* ES cells were cultured in the absence (–OHT, upper panels) or presence (+OHT, day 4, lower panels) of OHT, and were immunostained with antibodies to Oct3/4 (green) and Gata4 (red). The left-most panels show nuclei stained with Hoechst 33342 (blue); the right-most panels show merged images. Arrowheads indicate differentiated cells that express Gata4 but not Oct3/4. Arrows indicate feeder cells. Scale bars: 200 μm in C; 45 μm in F.

The above results demonstrate that Ring1A/B depletion converts the local chromatin from an inactive into an active configuration. This would suggest that the engagement of PRC1 is important to ensure robust silencing within chromatin domains that are predisposed to transcriptional activation (Azuara et al., 2006; Bernstein et al., 2006).

A large number of genes are repressed by both Ring1A/B and Oct3/4

Given that Ring1A/B are required for the maintenance of ES cell identity, we next examined the relationship between Ring1A/B and the core transcriptional regulatory circuitry in ES cells, because a previous study demonstrated that OCT3/4, SOX2 and NANOG co-occupy a significant subset of PRC2 target genes in human ES cells (Lee et al., 2006). In fact, inactive genes bound by OCT3/4, SOX2 and/or NANOG in human ES cells are overrepresented among those genes more than 2-fold derepressed in *Ring1A/B*-dKO mouse ES cells (see Fig. S4 in the supplementary material).

To directly test whether Ring1A/B mediate transcriptional silencing by the core transcriptional circuitry we made use of *Oct3/4* conditional knockout ES cells (ZHBTc4) (Niwa et al., 2000), comparing changes in gene expression in *Oct3/4*-KO and *Ring1A/B*-dKO cells. Because most *Oct3/4*-KO ES cells begin to exhibit trophectoderm-like morphology within 2 to 3 days after induction (Niwa et al., 2000), we analyzed RNA from ES cells 1 day after tetracycline (Tc) treatment, at which time Oct3/4 protein is extensively depleted, thus minimizing the contribution of secondary changes in gene expression resulting from differentiation. As controls, we also analyzed gene expression in *Eed*- and *Dnmt1*-KO ES cells. *Dnmt1*-KO ES cells self-renew but fail to undergo differentiation upon induction (Lei et al., 1996). Fold changes for respective probes determined against the parental cells were distributed on scatter diagrams and the correlation among respective KO ES cells was calculated (Fig. 3A). We found a strong correlation in total calculable genes between *Oct3/4*-KO and *Ring1A/B*-dKO ES cells (r=0.279). Overall gene expression in *Ring1A/B*-dKO ES cells also exhibited a strong correlation (r=0.359) with the *Eed*-KO, which might represent functional engagement of PRC1 and PRC2. By contrast, we found no correlation of the *Dnmt1*-KO with either the *Ring1A/B*-dKO (r=0.078) or *Oct3/4*-KO (r=–0.001). This analysis indicates that a large number of genes in ES cells are concurrently repressed by Oct3/4 and Ring1A/B.

Next we tested which genes regulated by Oct3/4 and Ring1A/B are important in maintaining ES cell identity. For this purpose, we extended the comparative gene expression analysis into sorted genes based on GO term categories. We found a comparable correlation in genes involved in regulation of transcription, transcription, development and apoptosis (Fig. 3B). Notably, the highest correlation was seen in genes involved in signaling pathways for Notch and Lif, both of which are implicated in stem cell maintenance (Androutsellis-Theotokis et al., 2006; Williams et al., 1988).

To test whether this observed correlation is statistically significant, we investigated the average expression changes caused by Ring1A/B depletion in genes more than 2-fold derepressed and repressed by Oct3/4 depletion. We further estimated the correlation of the expression changes with the degree of Ring1B binding to the respective genes. On average, derepressed genes in *Oct3/4*-KO cells were significantly derepressed in the *Ring1A/B*-dKO, as represented by a value at the zero point on the x-axis (P=1.23×10^{-39}) (Fig. 3C, red circle; see also Table S6 in the supplementary material). The degree of derepression in *Ring1A/B*-dKO showed a linear correlation with the degree of Ring1B binding (Fig. 3C, red circles). Concordantly, 120 out of 670 genes repressed by Oct3/4 were bound by Ring1B (Fig. 3D). By contrast, repressed genes in the *Oct3/4*-KO were only slightly repressed in the *Ring1A/B*-dKO, and these were genes that bound less Ring1B, whereas this was not the case at genes bound by Ring1B at intermediate or high levels (Fig. 3C, blue circles). Taken together with the spontaneous differentiation observed in *Ring1A/B*-dKO ES cells, Ring1A/B appear to be functionally linked with Oct3/4 in mediating ES cell identity.

Oct3/4 is required to engage PRC1 and PRC2 at target gene promoters

To examine the molecular basis for the functional link between Oct3/4 and Ring1A/B, we used ChIP to investigate the effect of Oct3/4 deletion on the levels of Ring1B at selected targets bound by both Ring1B and Oct3/4 and/or Nanog (Boyer et al., 2005; Loh et al., 2006). Of the selected genes *Cdx2*, *Hand1*, *Gata6* and *Hoxb4* were derepressed 1 day after Oct3/4 depletion, whereas *T*, *Otx2* and *Hoxb8* were not (Fig. 4A). Ring1B binding was significantly reduced irrespective of transcriptional status, suggesting Oct3/4-mediated regulation Ring1B binding to the chromatin (Fig. 4B). We extended the analysis to examine whether this hierarchical link is applicable to other Ring1B target genes by the ChIP-chip approach. As shown in Fig. 4C, Ring1B binding to the promoter regions of the target genes was, on average, significantly reduced 2 days after Tc treatment of ZHBTc4 ES cells. Therefore, binding of Ring1B to the chromatin in ES cells is generally dependent on Oct3/4. It has

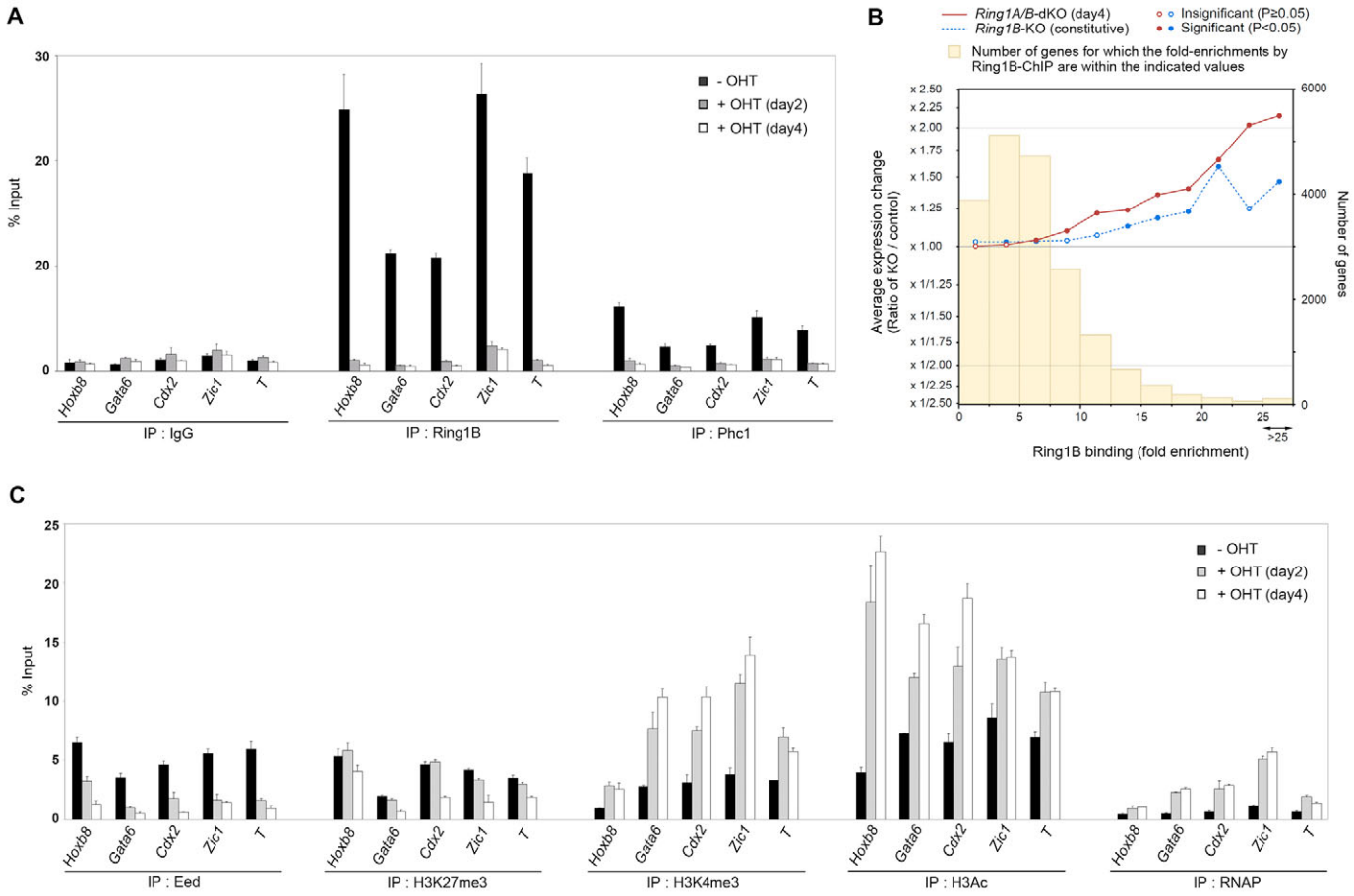

Fig. 2. Ring1A/B mediate repression of developmental regulators by inhibiting chromatin remodeling via direct binding. (**A**) Loss of Ring1B and Phc1 binding to the selected target promoter regions upon depletion of Ring1B in ES cells. Kinetics of local levels of Ring1B binding and Phc1 binding after OHT administration in *Ring1A*$^{-/-}$;*Ring1B*$^{fl/fl}$;*Rosa26*::*CreERT2* ES cells were determined by ChIP and site-specific real-time PCR. The relative amount of immunoprecipitated DNA is depicted as a percentage of input DNA. Error bars represent s.d. determined from at least three independent experiments. (**B**) Quantitative representation of the correlation between Ring1B binding and degree of derepression. Genes bound by Ring1B in their promoter regions in wild-type ES cells were identified by a ChIP-on-chip approach. Fold enrichment values for respective genes were calculated against the input and binned (each bin containing 2.5-fold enrichment). The number of genes in a bin (yellow bar) and the average change in expression from microarray analysis of *Ring1B*-KO (blue) and *Ring1A/B*-dKO (red) are indicated. Expression changes were statistically evaluated using Student's *t*-test under the null hypothesis that derepression was not observed. Significantly ($P<0.05$) derepressed bins and insignificant bins are indicated by solid and open circles, respectively. For actual values used to derive the graph and a list of Ring1B-bound genes, see Tables S4 and S5, respectively, in the supplementary material. (**C**) Changes in PRC2 binding and histone modification at Ring1B target loci following *Ring1A/B* depletion in ES cells. Kinetics of local levels of Eed, histone H3 lysine 27 trimethylation (H3K27me3), lysine 4 trimethylation (H3K4me3), lysine 9/14 acetylation (H3Ac), and non-phosphorylated RNA polymerase II (RNAPII) binding at the selected targets for Ring1B after OHT administration in *Ring1A*$^{-/-}$;*Ring1B*$^{fl/fl}$;*Rosa26*::*CreERT2* ES cells were determined by ChIP and site-specific real-time PCR. The relative amount of immunoprecipitated DNA is depicted as a percentage of input. Error bars represent s.d. determined from at least three independent experiments.

been reported that chromatin binding of Ring1B is also regulated by PRC2 functions (Boyer et al., 2006). We thus extended the analysis to address whether Oct3/4-dependent chromatin-binding of Ring1B involves PRC2, and found that binding of Eed to these genes was significantly reduced as well (Fig. 4B). Taken together, these results indicate that Oct3/4 mediates local engagement of PRC1 and PRC2.

Since enforced Ring1A/B depletion led to a rapid increase in the H3K4me3 level at the target genes (Fig. 2C), we next investigated changes in the degree of H3K4me3 at these genes upon Oct3/4 depletion. Notably, the level of H3K4me3 was increased at *Cdx2*, *Hand1*, *Gata6* and *Hoxb4*, whereas it was reduced or unchanged at *T*, *Otx2* and *Hoxb8*, consistent with increased gene expression (Fig. 4B). This indicates that the global reduction of PcG binding is not the sole mechanism for the changes in gene expression profile observed in ES cells upon Oct3/4 depletion. Oct3/4 has been suggested to upregulate some target genes and downregulate others. *Otx2* is one gene that has been experimentally verified to be upregulated directly by Oct3/4 (Boyer et al., 2005; Loh et al., 2006; Matoba et al., 2006). Moreover, the co-occupancy of promoters by PRC2 and OCT4/SOX2/NANOG has been demonstrated only at the transcriptionally repressed genes in human ES cells (Boyer et al., 2006). Considered together with the phenotypic difference between *Oct3/4*-KO and *Ring1A/B*-dKO ES cells, the global reduction in PcG binding might be a part of the mechanism for the differentiation of *Oct3/4*-KO ES cells.

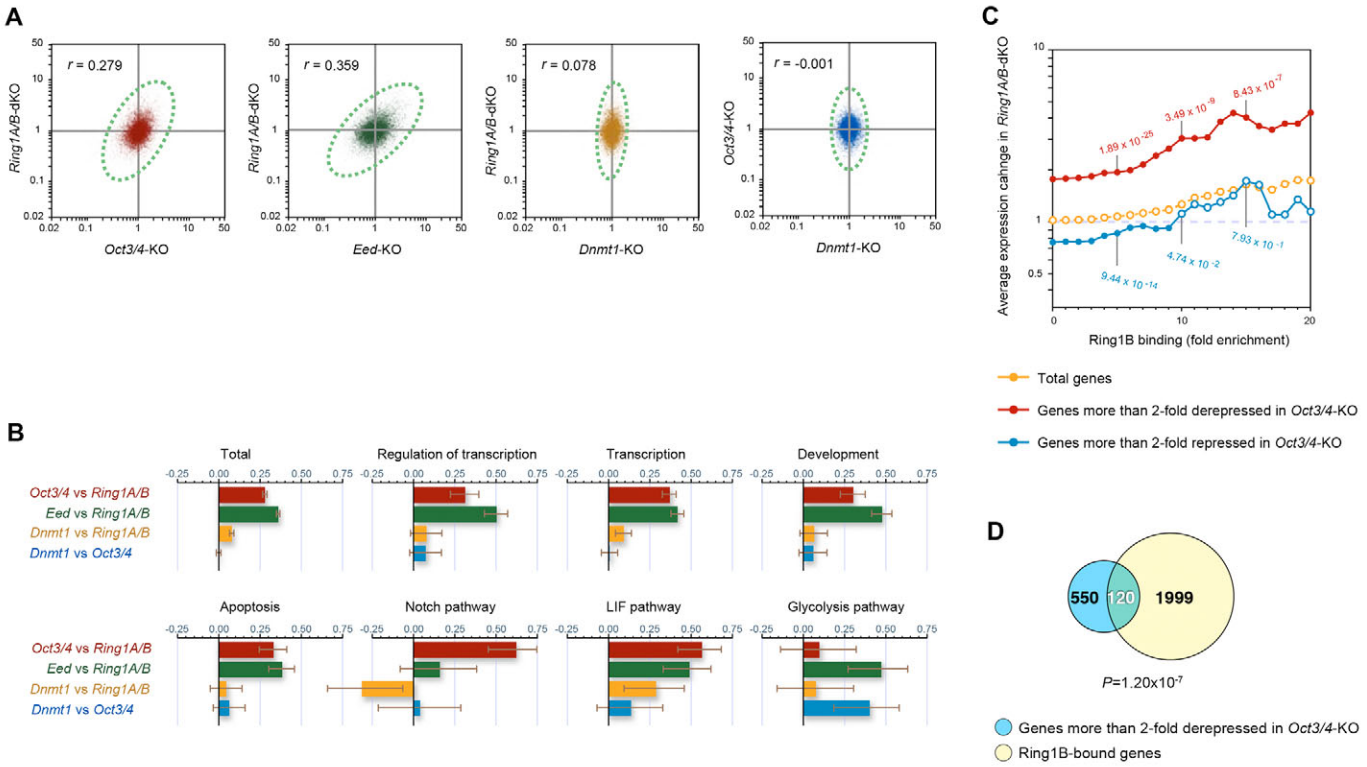

Fig. 3. Significant overlap of derepressed genes in *Ring1A/B*-dKO and *Oct3/4*-KO ES cells. (**A**) Scatter diagrams representing the correlation for changes in gene expression between respective KO ES cells. Each dot represents a specific probe. Fold changes of expression given by each probe in each KO against parental ES cells are dotted in the scatter diagram. Pearson's correlation coefficient (*r*) in each comparison is indicated in each panel. The distribution of dots is approximated by dotted ellipses. We prepared RNA from *Oct3/4*-KO ES cells 1 day after gene deletion was induced; *Ring1A/B*-dKO RNA was isolated at 4 days. Diagrams indicate the correlation of gene expression in *Eed*-KO versus *Ring1A/B*-dKO (green), *Oct3/4*-KO versus *Ring1AB*-dKO (red), *Dnmt1*-KO versus *Ring1A/B*-dKO (yellow), and *Dnmt1*-KO versus *Oct3/4*-KO (blue). (**B**) Pearson's correlation of expression changes for probes that belong to specific GO classifications are shown by bars. The same color codes are used as in A. Annotations are indicated above each graph. Error bars represent 95% confidence intervals of correlation coefficients calculated by Z transformation. (**C**) Graphical representation of correlation of derepressed genes in *Oct3/4*-KO and *Ring1A/B*-dKO ES cells in terms of the degree of Ring1B binding. Based on the genome-wide gene expression profiling, we first identified groups of genes more than 2-fold derepressed (red circles) or repressed (blue circles) in *Oct3/4*-KO ES cells. Average expression changes in *Ring1A/B*-dKO cells among those genes were plotted according to the degree of Ring1B binding determined by ChIP-chip and compared with the average of total genes (yellow circles). Where average expression changes in respective groups were statistically significant, relative to the total, the circles are solid; the open blue circles indicate that the difference from total genes is not statistically significant. *P*-values over 5-, 10- and 15-fold enrichment for Ring1B binding are shown. For actual values, see Table S6 in the supplementary material. (**D**) A significant fraction of the genes repressed by Oct3/4 is bound by Ring1B. The number of genes in each category of the Venn diagram is indicated.

Finally, we examined whether the binding of Oct3/4 depends on Ring1A/B. The levels of Oct3/4 binding to the PcG target sites were either unchanged or slightly decreased 2 to 4 days after OHT treatment of the *Ring1A/B*-dKO ES cells (Fig. 4D). Considering that the overall level of Oct3/4 decreases slightly 4 days after OHT treatment (see Fig. S3 in the supplementary material), we conclude that Ring1A/B are not directly required for the binding of Oct3/4 to the target sites.

In summary, loss of Oct3/4 consistently results in the reduction of Ring1B and Eed binding at PcG target genes in ES cells. Oct3/4 may maintain the repression of essential developmental regulators such as *Cdx2* and *Gata6* (Fujikura et al., 2002; Niwa et al., 2005) by maintaining local engagement of PRC1 and PRC2.

Molecular links between Polycomb and the core transcriptional regulatory circuitry

To determine the molecular mechanism for the global reduction of Ring1B binding upon Oct3/4 depletion, we investigated the effect of Oct3/4 deletion on the level of PRC1 and PRC2 proteins. Although Ring1B expression was only minimally affected during the first 48 hours of Tc treatment, expression of Phc1, Eed and Suz12 was significantly reduced (Fig. 5A). The decrease in Phc1 and PRC2 proteins was accompanied by a significant reduction in their respective transcript levels, whereas this was not the case for other PRC1 components, including *Ring1B* and *Bmi1* (Fig. 5B). Therefore, Oct3/4 regulates the expression of PRC1 and PRC2 components, and this may partly involve transcriptional regulation.

We also investigated whether the physical interaction of Ring1B with the Rex1 (Zfp42 – Mouse Genome Informatics) complex (Wang et al., 2006) could be extended to Oct3/4. Significant amounts of Oct3/4 and Ring1B as well as Rybp, a Ring1B-binding protein (Garcia et al., 1999), were found to form complexes in ES cells, whereas the PRC2 protein Suz12 did not co-immunoprecipitate with either Oct3/4 or Ring1B (Fig. 5C). Since reciprocal co-immunoprecipitation of Oct3/4 and Ring1B was not affected by the addition of ethidium bromide, which is known to

disrupt protein-DNA interactions without affecting protein-protein interactions (Lai and Herr, 1992) (Fig. 5C, right), this interaction is not mediated by genomic DNA. This result suggests that the local binding of PRC1 to chromatin might involve direct interactions between PRC1 and protein complexes that include Nanog and/or Oct3/4. Taken together, these results suggest that PRC1 is linked to the core transcriptional regulatory circuitry at multiple levels.

PRC1/2 binding is significantly reduced by Gata6 overexpression in ES cells

We went on to address whether PRC1/2 binding depends solely on Oct3/4 or on the regulatory system for ES cell self-renewal. Various differentiation cues have been demonstrated to disrupt ES cell self-renewal maintained by the core transcriptional regulatory circuitry. For example, Gata6 has been thought of as a downstream effector of Nanog, and enforced Gata6 expression induces the differentiation program towards extraembryonic endoderm (Chazaud et al., 2006; Fujikura et al., 2002). We therefore examined the effects of the enforced expression of Gata6 on PRC1/2 engagement at Ring1B targets using ES cells expressing a Gata6-GR fusion protein (G6GR) (Shimosato et al., 2007). As previously described, G6GR cells rapidly lose ES-cell-like morphology and show dispersed visceral endoderm-like morphology upon Gata6 activation by the administration of dexamethasone (Dex) (see Fig. S5 in the supplementary material).

We first analyzed the effect of Gata6 activation on the level of PRC1 and PRC2 proteins (Fig. 6A). The level of Ring1B protein was unaffected or only minimally affected during the first 2 days of Dex treatment, but was slightly decreased by day 3. The levels of Phc1, Ezh2, Eed and Suz12 proteins were significantly reduced after Dex treatment, whereas H3K27me3 was unaffected.

Next we used microarray analysis to evaluate the effect of enforced Gata6 expression on gene expression, and compared this profile with those of *Oct3/4*-KO and *Ring1A/B*-dKO ES cells. We found a comparable correlation between Gata6-differentiated and *Ring1A/B*-dKO ES cells (r=0.297), between *Oct3/4*-KO and Gata6-differentiated ES cells (r=0.318), and between *Oct3/4*-KO and *Ring1A/B*-dKO ES cells (r=0.279), not only in terms of total calculable genes but also in genes involved in development,

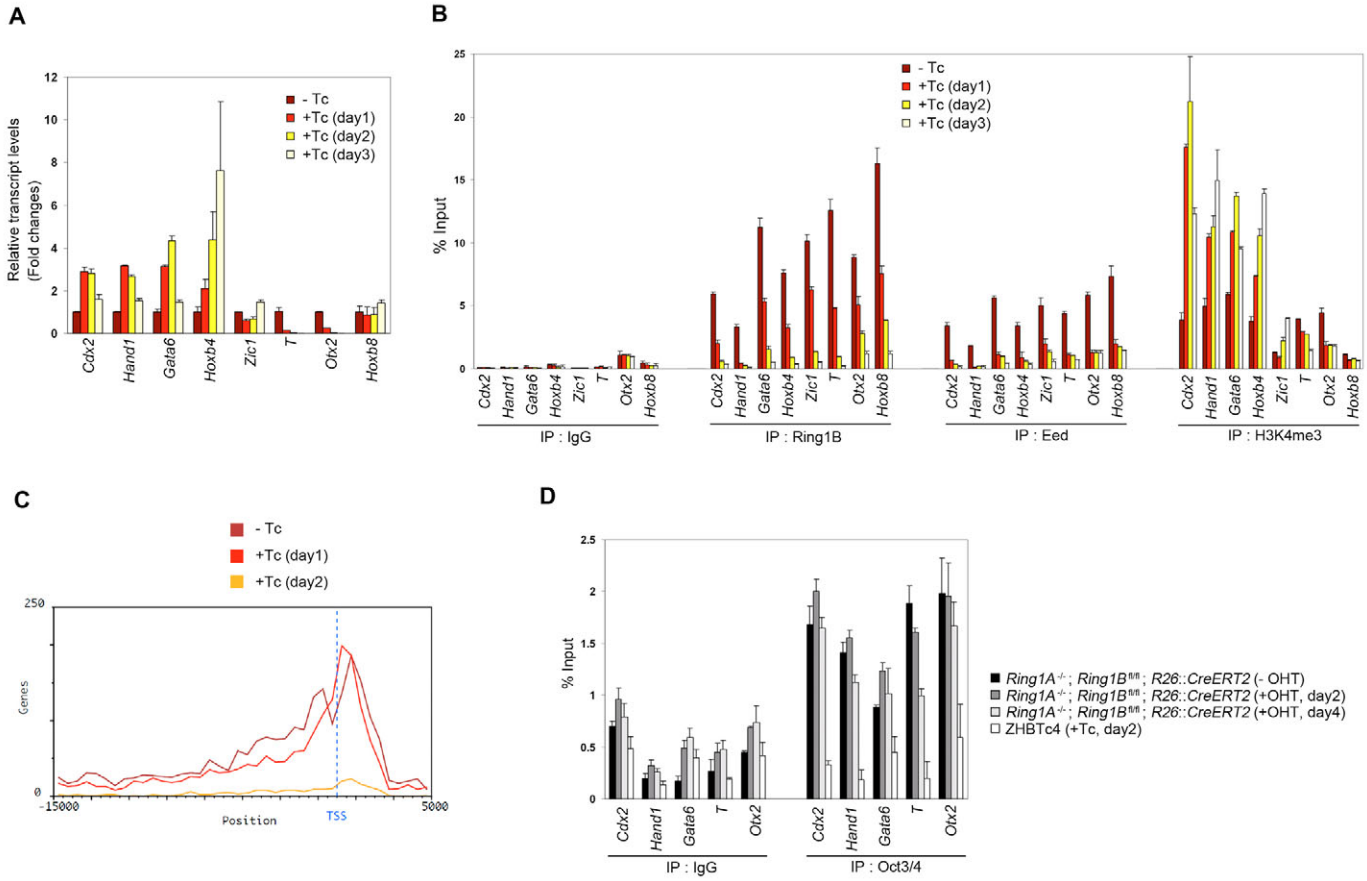

Fig. 4. Oct3/4 is required to engage PRC1 and PRC2 at target gene promoters. (**A**) Changes in expression levels for the selected Ring1B target genes after tetracycline treatment of ZHBTc4 ES cells were determined as described in Fig. 1E. (**B**) ChIP analysis showing binding of Ring1B and Eed and levels of H3K4me3 at the promoter regions of the selected target genes after tetracycline treatment of ZHBTc4 ES cells. The relative amount of immunoprecipitated DNA is depicted as a percentage of input. Error bars represent s.d. determined from at least three independent experiments. (**C**) ChIP-on-chip analysis showing the average Ring1B binding to the promoter regions (from –8 kb to +2 kb relative to the transcription start sites) of the target genes before and after conditional deletion of *Oct3/4*. (**D**) ChIP analysis showing binding of Oct3/4 at the promoter regions of the selected target genes after OHT treatment of *Ring1A*$^{-/-}$;*Ring1B*$^{fl/fl}$;*Rosa26*::*CreERT2* ES cells. The relative amount of immunoprecipitated DNA is depicted as a percentage of input. Error bars represent s.d. determined from at least three independent experiments.

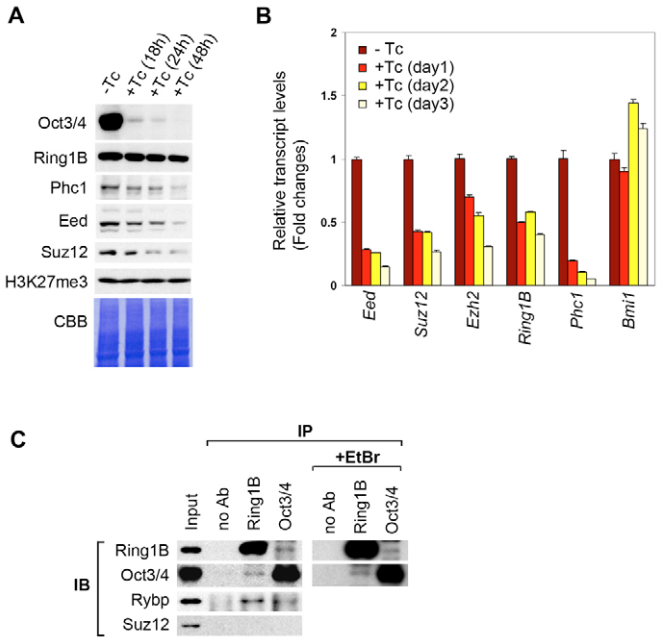

Fig. 5. Possible mechanisms for the reduction in Ring1B binding upon Oct3/4 depletion or differentiation cues. (**A**) Western blot demonstrating changes in the levels of Oct3/4, Ring1B, Phc1, Eed, Suz12 and H3K27me3 after conditional deletion of *Oct3/4* by tetracycline (Tc) treatment of ZHBTc4 ES cells. (**B**) Changes in gene expression levels for *Eed*, *Suz12*, *Ezh2*, *Ring1B*, *Phc1* and *Bmi1* after tetracycline treatment (+Tc) of ZHBTc4 ES cells were determined by real-time PCR, normalized to an *Actb* control and depicted as fold changes relative to the tetracycline-untreated (–Tc) ES cells. Error bars are based on the s.d. derived from triplicate PCR reactions. (**C**) Physical interaction of Ring1B and Oct3/4 in wild-type ES cells demonstrated by reciprocal immunoprecipitation/immunoblot analyses. Antibodies used for immunoprecipitation (IP, top) and immunoblotting (IB, side) are indicated. The association between Ring1B and Oct3/4 proteins remains intact in the presence of ethidium bromide (+EtBr), a DNA-intercalating drug that can disassociate proteins from DNA.

transcription, apoptosis and cell cycle (Fig. 6B). Therefore, a subset of genes induced by enforced Gata6 activation is correlated with those regulated by Oct3/4 and Ring1A/B, suggesting an extension of the functional link to Gata6.

We then investigated whether Gata6 activation affects the levels of Ring1B and Eed at selected Polycomb targets. Of the selected genes, the expression level was increased for *Gata6*, *Cdx2*, *Zic1* and *T*, whereas it was reduced or unchanged for *Hoxb8* and *Hand1* upon Gata6 expression (data not shown). Ring1B binding was significantly reduced irrespective of transcriptional status (Fig. 6C). Phc1 and Eed binding was also reduced (Fig. 6C), consistent with the observed reduction in protein levels (Fig. 6A). These results indicate that Gata6 activation impacts upon gene expression in similar manner to Oct3/4 depletion. Therefore, it is likely that the local engagement of PRC1 depends on the core transcriptional regulatory circuitry rather than solely on Oct3/4 in ES cells.

DISCUSSION

In this study, we first demonstrate that Ring1A/B are required to maintain ES cells in an undifferentiated state by repressing the expression of developmental regulators that direct differentiation of ES cells. This process involves local inhibition of chromatin remodeling via direct binding of PRC1. We further show that Ring1A/B-mediated PcG silencing is hierarchically linked to the core transcriptional regulatory circuitry and that this linkage can be abolished by developmental cues that negatively regulate the core circuitry (Fig. 7). Developmental regulators repressed by this epistatic link, such as *Cdx2* and *Gata6*, are shown to be predisposed for active transcription. Active and reversible repression by this epistatic link is important to potentiate ES cells so that they can respond to developmental cues appropriately and, consequently, it may underpin the maintenance of pluripotency. Therefore, our data show that Ring1A/B are instrumental for the core transcriptional regulatory circuitry to maintain ES cell identity.

The dissociation of PRC1 as a prerequisite for subsequent association of chromatin remodeling components

These and previous studies suggest that PcG proteins are linked to the core transcriptional regulatory circuitry at multiple levels (Fig. 3) (Lee et al., 2006). Oct3/4 is likely to recruit Ring1B to its targets via direct interactions and also to induce the expression of PRC1 components via a transcriptional regulatory mechanism (Fig. 5). Moreover, it is notable that Oct3/4 loss displaces Ring1B from most of its target genes, which are not necessarily functional targets of Oct3/4 (Fig. 4C). This prompts us to postulate an activity that modulates Ring1B recruitment under the regulation of Oct3/4. Indeed, the RING1 and YY1 binding protein, Rybp, potentially fulfils such a linking role between Oct3/4 and Ring1B because Rybp is able to form complexes with both proteins (Fig. 5C) (Wang et al., 2006). Such multiple interactions might enable coordinated displacement of PRC1 and PRC2 from their target genes upon disruption of the core circuitry by differentiation cues. Since forced depletion of *Ring1A/B* leads to spontaneous differentiation of ES cells, dissociation of PRC1 from the targets may be functionally implicated in the differentiation process. We presume that the dissociation of PRC1 and PRC2 is a prerequisite for the subsequent association of other chromatin modifiers such as Trithorax group proteins, which catalyze local hypertrimethylation of H3K4 upon Oct3/4 depletion (Dou et al., 2005; Wysocka et al., 2003). This is supported by our results shown in Fig. 2C, and by previous experiments showing that the SWI-SNF complex is unable to remodel polynucleosomal templates bound by PRC1 in vitro (Shao et al., 1999). Therefore, the global enhancement of chromatin remodeling at developmental genes might be one of the essential events in promoting proper differentiation of ES cells.

Implications from the reversibility of Polycomb binding in the balance of self-renewal versus differentiation

The reversibility of Polycomb binding to the targets regulated by the core transcriptional regulatory circuitry and by differentiation cues might confer self-renewing and differentiation capacities to ES cells. Intriguingly, PcG silencing has been suggested to be involved in the function and maintenance of tissue stem and cancer cells, which are also characterized by both self-renewal and differentiation potency (Lessard and Sauvageau, 2003; Molofsky et al., 2003; Ohta et al., 2002; Park et al., 2003; Villa et al., 2007). For example, *Bmi1* loss promotes differentiation of hematopoietic stem cells (HSCs) and premature senescence of neural stem cells, whereas forced expression of *Bmi1* enhances symmetrical cell division of HSCs (Iwama et al., 2004; Molofsky et al., 2005).

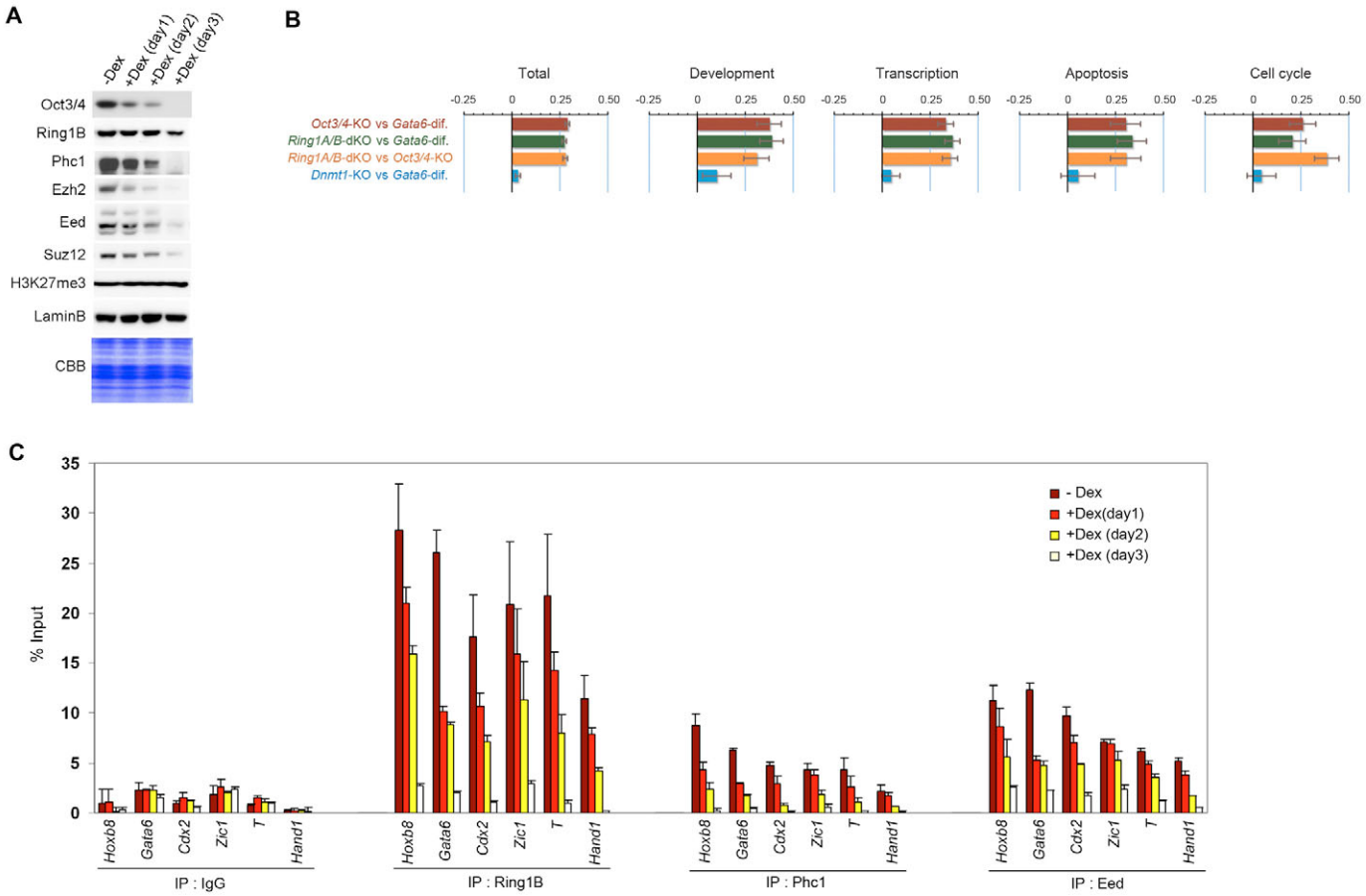

Fig. 6. The engagement of PRC1 and PRC2 is gradually decreased upon Gata6-mediated differentiation of ES cells into primitive endoderm lineages. (**A**) Western blot analysis demonstrating changes in the levels of Oct3/4, Ring1B, Phc1, Ezh2, Eed, Suz12 and H3K27me3 after conditional activation of Gata6 by dexamethasone (Dex) treatment of G6GR ES cells. Lamin B and CBB staining confirmed equal loading. (**B**) Significant overlap of expression profiles in *Ring1A/B*-dKO (day 4), *Oct3/4*-KO (day 1) and Gata6-differentiated (day 2) ES cells. Pearson's correlation of expression changes for probes that belong to specific GO classifications are shown by bars. Functional groupings are indicated above each graph. Error bars represent 95% confidence intervals of correlation coefficients calculated by Z transformation. (**C**) ChIP analysis showing binding of Ring1B, Phc1 and Eed at the promoter regions of the selected target genes after Dex treatment in G6GR ES cells. The relative amount of immunoprecipitated DNA is depicted as a percentage of input. Error bars represent s.d. determined from at least three independent experiments.

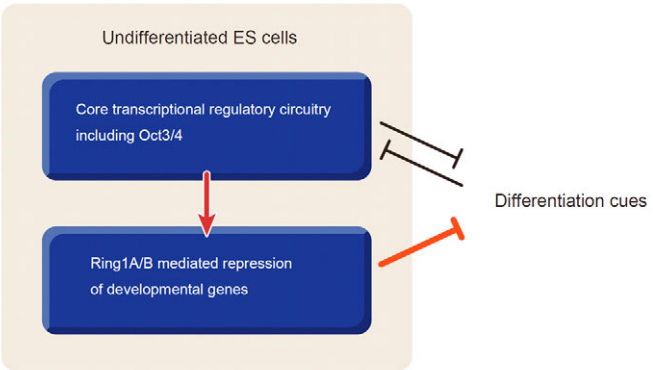

Fig. 7. Schematic representation of the interaction between Ring1A/B and the core transcriptional regulatory circuitry in mouse ES cells. Ring1A/B-mediated PcG silencing functions downstream of the core transcriptional regulatory circuitry including Oct3/4. Developmental cues, such as *Gata6* activation, downregulate the activity of the core transcriptional regulatory circuitry, which accompanies a global decrease in PcG silencing.

Recently, it has been reported that knockdown of *SUZ12* in acute promyelocytic leukemic cells results in myeloid differentiation (Villa et al., 2007). It is thus likely that similar molecular mechanisms identified in ES cells that involve *Ring1A/B* might operate in the maintenance and differentiation of various tissue stem cells and cancer cells. Since *Oct3/4* and *Nanog* are not expressed in most somatic cells, other downstream effectors expressed in common among the stem cells might be more directly involved in the regulation of Polycomb binding. Alternatively, other factors specifically expressed in tissue and/or cancer stem cells might substitute for the action of *Oct3/4* or *Nanog*. Further studies will be needed to clarify these issues.

We thank Hitoshi Niwa for providing ZHBTc4, G6GR and ZHTc6 cells. This work was supported in part by a grant from the Genome Network Project (to H.K.) and a grant-in-aid for Scientific Research on Priority Areas (17045038, to M.E.) from the Ministry of Education, Culture, Sports, Science and Technology, Japan.

Supplementary material

Supplementary material for this article is available at http://dev.biologists.org/cgi/content/full/135/8/1513/DC1

References

Androutsellis-Theotokis, A., Leker, R. R., Soldner, F., Hoeppner, D. J., Ravin, R., Poser, S. W., Rueger, M. A., Bae, S. K., Kittappa, R. and McKay, R. D. (2006). Notch signalling regulates stem cell numbers in vitro and in vivo. *Nature* **442**, 823-826.

Atsuta, T., Fujimura, S., Moriya, H., Vidal, M., Akasaka, T. and Koseki, H. (2001). Production of monoclonal antibodies against mammalian Ring1B proteins. *Hybridoma* **20**, 43-46.

Auernhammer, C. J. and Melmed, S. (2000). Leukemia-inhibitory factor-neuroimmune modulator of endocrine function. *Endocr. Rev.* **21**, 313-345.

Avilion, A. A., Nicolis, S. K., Pevny, L. H., Perez, L., Vivian, N. and Lovell-Badge, R. (2003). Multipotent cell lineages in early mouse development depend on SOX2 function. *Genes Dev.* **17**, 126-140.

Azuara, V., Perry, P., Sauer, S., Spivakov, M., Jorgensen, H. F., John, R. M., Gouti, M., Casanova, M., Warnes, G., Merkenschlager, M. et al. (2006). Chromatin signatures of pluripotent cell lines. *Nat. Cell Biol.* **8**, 532-538.

Bernstein, B. E., Mikkelsen, T. S., Xie, X., Kamal, M., Huebert, D. J., Cuff, J., Fry, B., Meissner, A., Wernig, M., Plath, K. et al. (2006). A bivalent chromatin structure marks key developmental genes in embryonic stem cells. *Cell* **125**, 315-326.

Bolstad, B. M., Irizarry, R. A., Astrand, M. and Speed, T. P. (2003). A comparison of normalization methods for high density oligonucleotide array data based on variance and bias. *Bioinformatics* **19**, 185-193.

Boyer, L. A., Lee, T. I., Cole, M. F., Johnstone, S. E., Levine, S. S., Zucker, J. P., Guenther, M. G., Kumar, R. M., Murray, H. L., Jenner, R. G. et al. (2005). Core transcriptional regulatory circuitry in human embryonic stem cells. *Cell* **122**, 947-956.

Boyer, L. A., Plath, K., Zeitlinger, J., Brambrink, T., Medeiros, L. A., Lee, T. I., Levine, S. S., Wernig, M., Tajonar, A., Ray, M. K. et al. (2006). Polycomb complexes repress developmental regulators in murine embryonic stem cells. *Nature* **441**, 349-353.

Buchwald, G., van der Stoop, P., Weichenrieder, O., Perrakis, A., van Lohuizen, M. and Sixma, T. K. (2006). Structure and E3-ligase activity of the Ring-Ring complex of polycomb proteins Bmi1 and Ring1b. *EMBO J.* **25**, 2465-2474.

Burdon, T., Smith, A. and Savatier, P. (2002). Signalling, cell cycle and pluripotency in embryonic stem cells. *Trends Cell Biol.* **12**, 432-438.

Cales, C., Roman-Trufero, M., Pavon, L., Serrano, I., Melgar, T., Endoh, M., Perez, C., Koseki, H. and Vidal, M. (2008). Inactivation of the polycomb group protein Ring1B unveils an antiproliferative role in hematopoietic cell expansion and cooperation with tumorigenesis associated with Ink4a deletion. *Mol. Cell. Biol.* **28**, 1018-1028.

Cao, R., Wang, L., Wang, H., Xia, L., Erdjument-Bromage, H., Tempst, P., Jones, R. S. and Zhang, Y. (2002). Role of histone H3 lysine 27 methylation in Polycomb-group silencing. *Science* **298**, 1039-1043.

Catena, R., Tiveron, C., Ronchi, A., Porta, S., Ferri, A., Tatangelo, L., Cavallaro, M., Favaro, R., Ottolenghi, S., Reinbold, R. et al. (2004). Conserved POU binding DNA sites in the Sox2 upstream enhancer regulate gene expression in embryonic and neural stem cells. *J. Biol. Chem.* **279**, 41846-41857.

Chambers, I., Colby, D., Robertson, M., Nichols, J., Lee, S., Tweedie, S. and Smith, A. (2003). Functional expression cloning of Nanog, a pluripotency sustaining factor in embryonic stem cells. *Cell* **113**, 643-655.

Chazaud, C., Yamanaka, Y., Pawson, T. and Rossant, J. (2006). Early lineage segregation between epiblast and primitive endoderm in mouse blastocysts through the Grb2-MAPK pathway. *Dev. Cell* **10**, 615-624.

Czermin, B., Melfi, R., McCabe, D., Seitz, V., Imhof, A. and Pirrotta, V. (2002). Drosophila enhancer of Zeste/ESC complexes have a histone H3 methyltransferase activity that marks chromosomal Polycomb sites. *Cell* **111**, 185-196.

Dou, Y., Milne, T. A., Tackett, A. J., Smith, E. R., Fukuda, A., Wysocka, J., Allis, C. D., Chait, B. T., Hess, J. L. and Roeder, R. G. (2005). Physical association and coordinate function of the H3 K4 methyltransferase MLL1 and the H4 K16 acetyltransferase MOF. *Cell* **121**, 873-885.

de Napoles, M., Mermoud, J. E., Wakao, R., Tang, Y. A., Endoh, M., Appanah, R., Nesterova, T. B., Silva, J., Otte, A. P., Vidal, M. et al. (2004). Polycomb group proteins Ring1A/B link ubiquitylation of histone H2A to heritable gene silencing and X inactivation. *Dev. Cell* **7**, 663-676.

del Mar Lorente, M., Marcos-Gutierrez, C., Perez, C., Schoorlemmer, J., Ramirez, A., Magin, T. and Vidal, M. (2000). Loss- and gain-of-function mutations show a polycomb group function for Ring1A in mice. *Development* **127**, 5093-5100.

Evans, M. J. and Kaufman, M. H. (1981). Establishment in culture of pluripotential cells from mouse embryos. *Nature* **292**, 154-156.

Fischle, W., Wang, Y., Jacobs, S. A., Kim, Y., Allis, C. D. and Khorasanizadeh, S. (2003). Molecular basis for the discrimination of repressive methyl-lysine marks in histone H3 by Polycomb and HP1 chromodomains. *Genes Dev.* **17**, 1870-1881.

Fujikura, J., Yamato, E., Yonemura, S., Hosoda, K., Masui, S., Nakao, K., Miyazaki, J.-i., and Niwa, H. (2002). Differentiation of embryonic stem cells is induced by GATA factors. *Genes Dev.* **16**, 784-789.

Fujimura, Y., Isono, K., Vidal, M., Endoh, M., Kajita, H., Mizutani-Koseki, Y., Takihara, Y., van Lohuizen, M., Otte, A., Jenuwein, T. et al. (2006). Distinct roles of Polycomb group gene products in transcriptionally repressed and active domains of Hoxb8. *Development* **133**, 2371-2381.

Garcia, E., Marcos-Gutierrez, C., del Mar Lorente, M., Moreno, J. C. and Vidal, M. (1999). RYBP, a new repressor protein that interacts with components of the mammalian Polycomb complex, and with the transcription factor YY1. *EMBO J.* **18**, 3404-3418.

Hamer, K. M., Sewalt, R. G., den Blaauwen, J. L., Hendrix, T., Satijn, D. P. and Otte, A. P. (2002). A panel of monoclonal antibodies against human polycomb group proteins. *Hybrid Hybridomics* **21**, 245-252.

Heinrich, P. C., Behrmann, I., Haan, S., Hermanns, H. M., Muller-Newen, G. and Schaper, F. (2003). Principles of interleukin (IL)-6-type cytokine signalling and its regulation. *Biochem. J.* **374**, 1-20.

Isono, K., Fujimura, Y.-i, Shinga, J., Yamaki, M., O-Wang, J., Takihara, Y., Murahashi, Y., Takada, Y., Mizutani-Koseki, Y. and Koseki, H. (2005a). Mammalian polyhomeotic homologues Phc2 and Phc1 act in synergy to mediate polycomb repression of Hox genes. *Mol. Cell. Biol.* **25**, 6694-6706.

Isono, K., Mizutani-Koseki, Y., Komori, T., Schmidt-Zachmann, M. S. and Koseki, H. (2005b). Mammalian polycomb-mediated repression of Hox genes requires the essential spliceosomal protein Sf3b1. *Genes Dev.* **19**, 536-541.

Iwama, A., Oguro, H., Negishi, M., Kato, Y., Morita, Y., Tsukui, H., Ema, H., Kamijo, T., Katoh-Fukui, Y., Koseki, H. et al. (2004). Enhanced self-renewal of hematopoietic stem cells mediated by the polycomb gene product Bmi-1. *Immunity* **21**, 843-851.

Kuroda, T., Tada, M., Kubota, H., Kimura, H., Hatano, S. Y., Suemori, H., Nakatsuji, N. and Tada, T. (2005). Octamer and Sox elements are required for transcriptional cis regulation of Nanog gene expression. *Mol. Cell. Biol.* **25**, 2475-2485.

Kuzmichev, A., Nishioka, K., Erdjument-Bromage, H., Tempst, P. and Reinberg, D. (2002). Histone methyltransferase activity associated with a human multiprotein complex containing the Enhancer of Zeste protein. *Genes Dev.* **16**, 2893-2905.

Lai, J. S. and Herr, W. (1992). Ethidium bromide provides a simple tool for identifying genuine DNA-independent protein associations. *Proc. Natl. Acad. Sci. USA* **89**, 6958-6962.

Lee, T. I., Jenner, R. G., Boyer, L. A., Guenther, M. G., Levine, S. S., Kumar, R. M., Chevalier, B., Johnstone, S. E., Cole, M. F., Isono, K. et al. (2006). Control of developmental regulators by Polycomb in human embryonic stem cells. *Cell* **125**, 301-313.

Leeb, M. and Wutz, A. (2007). Ring1B is crucial for the regulation of developmental control genes and PRC1 proteins but not X inactivation in embryonic cells. *J. Cell Biol.* **178**, 219-229.

Lei, H., Oh, S. P., Okano, M., Juttermann, R., Goss, K. A., Jaenisch, R. and Li, E. (1996). De novo DNA cytosine methyltransferase activities in mouse embryonic stem cells. *Development* **122**, 3195-3205.

Lessard, J. and Sauvageau, G. (2003). Bmi-1 determines the proliferative capacity of normal and leukaemic stem cells. *Nature* **423**, 255-260.

Loh, Y. H., Wu, Q., Chew, J. L., Vega, V. B., Zhang, W., Chen, X., Bourque, G., George, J., Leong, B., Liu, J. et al. (2006). The Oct4 and Nanog transcription network regulates pluripotency in mouse embryonic stem cells. *Nat. Genet.* **38**, 431-440.

Martin, G. R. (1981). Isolation of a pluripotent cell line from early mouse embryos cultured in medium conditioned by teratocarcinoma stem cells. *Proc. Natl. Acad. Sci. USA* **78**, 7634-7638.

Matoba, R., Niwa, H., Masui, S., Ohtsuka, S., Carter, M. G., Sharov, A. A. and Ko, M. S. (2006). Dissecting oct3/4-regulated gene networks in embryonic stem cells by expression profiling. *PLoS ONE* **1**, e26.

Min, J., Zhang, Y. and Xu, R. M. (2003). Structural basis for specific binding of Polycomb chromodomain to histone H3 methylated at Lys 27. *Genes Dev.* **17**, 1823-1828.

Mitsui, K., Tokuzawa, Y., Itoh, H., Segawa, K., Murakami, M., Takahashi, K., Maruyama, M., Maeda, M. and Yamanaka, S. (2003). The homeoprotein Nanog is required for maintenance of pluripotency in mouse epiblast and ES cells. *Cell* **113**, 631-642.

Miyagishima, H., Isono, K., Fujimura, Y., Iyo, M., Takihara, Y., Masumoto, H., Vidal, M. and Koseki, H. (2003). Dissociation of mammalian Polycomb-group proteins, Ring1B and Rae28/Ph1, from the chromatin correlates with configuration changes of the chromatin in mitotic and meiotic prophase. *Histochem. Cell Biol.* **120**, 111-119.

Molofsky, A. V., Pardal, R., Iwashita, T., Park, I. K., Clarke, M. F. and Morrison, S. J. (2003). Bmi-1 dependence distinguishes neural stem cell self-renewal from progenitor proliferation. *Nature* **425**, 962-967.

Molofsky, A. V., He, S., Bydon, M., Morrison, S. J. and Pardal, R. (2005). Bmi-1 promotes neural stem cell self-renewal and neural development but not mouse growth and survival by repressing the p16Ink4a and p19Arf senescence pathways. *Genes Dev.* **19**, 1432-1437.

Muller, J., Hart, C. M., Francis, N. J., Vargas, M. L., Sengupta, A., Wild, B., Miller, E. L., O'Connor, M. B., Kingston, R. E. and Simon, J. A. (2002).

Histone methyltransferase activity of a Drosophila Polycomb group repressor complex. *Cell* **111**, 197-208.
Nichols, J., Zevnik, B., Anastassiadis, K., Niwa, H., Klewe-Nebenius, D., Chambers, I., Scholer, H. and Smith, A. (1998). Formation of pluripotent stem cells in the mammalian embryo depends on the POU transcription factor Oct4. *Cell* **95**, 379-391.
Niwa, H., Miyazaki, J. and Smith, A. G. (2000). Quantitative expression of Oct-3/4 defines differentiation, dedifferentiation or self-renewal of ES cells. *Nat. Genet.* **24**, 372-376.
Niwa, H., Toyooka, Y., Shimosato, D., Strumpf, D., Takahashi, K., Yagi, R. and Rossant, J. (2005). Interaction between Oct3/4 and Cdx2 determines trophectoderm differentiation. *Cell* **123**, 917-929.
Ohta, H., Sawada, A., Kim, J. Y., Tokimasa, S., Nishiguchi, S., Humphries, R. K., Hara, J. and Takihara, Y. (2002). Polycomb group gene rae28 is required for sustaining activity of hematopoietic stem cells. *J. Exp. Med.* **195**, 759-770.
Okumura-Nakanishi, S., Saito, M., Niwa, H. and Ishikawa, F. (2005). Oct-3/4 and Sox2 regulate Oct-3/4 gene in embryonic stem cells. *J. Biol. Chem.* **280**, 5307-5317.
Orlando, V., Strutt, H. and Paro, R. (1997). Analysis of chromatin structure by in vivo formaldehyde cross-linking. *Methods* **11**, 205-214.
Park, I. K., Qian, D., Kiel, M., Becker, M. W., Pihalja, M., Weissman, I. L., Morrison, S. J. and Clarke, M. F. (2003). Bmi-1 is required for maintenance of adult self-renewing haematopoietic stem cells. *Nature* **423**, 302-305.
Rodda, D. J., Chew, J. L., Lim, L. H., Loh, Y. H., Wang, B., Ng, H. H. and Robson, P. (2005). Transcriptional regulation of nanog by OCT4 and SOX2. *J. Biol. Chem.* **280**, 24731-24737.
Seibler, J., Zevnik, B., Kuter-Luks, B., Andreas, S., Kern, H., Hennek, T., Rode, A., Heimann, C., Faust, N., Kauselmann, G. et al. (2003). Rapid generation of inducible mouse mutants. *Nucleic Acids Res.* **31**, e12.
Shao, Z., Raible, F., Mollaaghababa, R., Guyon, J. R., Wu, C. T., Bender, W. and Kingston, R. E. (1999). Stabilization of chromatin structure by PRC1, a Polycomb complex. *Cell* **98**, 37-46.
Shimosato, D., Shiki, M. and Niwa, H. (2007). Extra-embryonic endoderm cells derived from ES cells induced by GATA Factors acquire the character of XEN cells. *BMC Dev Biol.* **7**, 80.
Villa, R., Pasini, D., Gutierrez, A., Morey, L., Occhionorelli, M., Vire, E., Nomdedeu, J. F., Jenuwein, T., Pelicci, P. G., Minucci, S. et al. (2007). Role of the polycomb repressive complex 2 in acute promyelocytic leukemia. *Cancer Cell* **11**, 513-525.
Wang, H., Wang, L., Erdjument-Bromage, H., Vidal, M., Tempst, P., Jones, R. S. and Zhang, Y. (2004). Role of histone H2A ubiquitination in Polycomb silencing. *Nature* **431**, 873-878.
Wang, J., Rao, S., Chu, J., Shen, X., Levasseur, D. N., Theunissen, T. W. and Orkin, S. H. (2006). A protein interaction network for pluripotency of embryonic stem cells. *Nature* **444**, 364-368.
Williams, R. L., Hilton, D. J., Pease, S., Willson, T. A., Stewart, C. L., Gearing, D. P., Wagner, E. F., Metcalf, D., Nicola, N. A. and Gough, N. M. (1988). Myeloid leukaemia inhibitory factor maintains the developmental potential of embryonic stem cells. *Nature* **336**, 684-687.
Wysocka, J., Myers, M. P., Laherty, C. D., Eisenman, R. N. and Herr, W. (2003). Human Sin3 deacetylase and trithorax-related Set1/Ash2 histone H3-K4 methyltransferase are tethered together selectively by the cell-proliferation factor HCF-1. *Genes Dev.* **17**, 896-911.

Table S1. Gene ontology analysis of derepressed genes by *Ring1B*-KO or *Ring1A/B*-dKO in ES cells

Derepressed genes by *Ring1A/B*-dKO (4 days after OHT treatment)

Category	GO description	*P* value
Biological process	Development	2.3E-29
	Regulation of transcription	8.0E-17
	Pattern specification	1.1E-14
	Cell adhesion	1.2E-14
	Signal transduction	1.1E-13
	Organ morphogenesis	1.0E-11
	G-protein coupled receptor protein signaling pathway	1.9E-11
	Immune response	4.3E-10
	Antigen processing and presentation of endogenous antigen	3.2E-09
	Antigen processing and presentation of endogenous peptide antigen via MHC class I	8.6E-09
	Ion transport	1.3E-08
	Transmembrane receptor protein tyrosine kinase signaling pathway	1.7E-08
	Phosphate transport	7.9E-08
	Axon guidance	8.5E-08
	Cell fate commitment	3.3E-07
Molecular function	Sequence-specific DNA binding	1.2E-23
	Receptor activity	2.2E-23
	Transcription factor activity	4.2E-23
	Ion channel activity	4.3E-13
	Calcium ion binding	1.8E-12
	Signal transducer activity	5.3E-12
	Voltage-gated ion channel activity	2.3E-10
	G-protein coupled receptor activity	2.1E-09
	GPI anchor binding	2.8E-09
	Structural molecule activity	3.2E-09
	Rhodopsin-like receptor activity	1.0E-08
	Extracellular matrix structural constituent conferring tensile strength	4.8E-08
	MHC class I receptor activity	6.2E-08
Cellular component	Extracellular space	9.0E-58
	Membrane	1.6E-31
	Integral to membrane	4.3E-30
	Extracellular matrix (sensu Metazoa)	5.5E-24
	Extracellular region	5.1E-23
	Transcription factor complex	2.3E-19
	Integral to plasma membrane	9.3E-14
	Collagen	6.3E-09
	External side of plasma membrane	3.2E-08
	Plasma membrane	6.2E-08
	MHC class I protein complex	4.2E-07

Derepressed genes by *Ring1B*-KO (4 days after OHT treatment)

Category	GO description	*P* value
Biological process	Development	6.7E-14
	Pattern specification	4.4E-12
	Immune response	3.0E-11
	Organ morphogenesis	1.6E-10
	Ion transport	8.8E-10
	Signal transduction	1.8E-08
	Defense response	2.9E-08
	Regulation of transcription	2.7E-07
	Cell adhesion	3.6E-07
Molecular function	Receptor activity	1.4E-17
	Sequence-specific DNA binding	5.9E-12
	Ion channel activity	1.1E-11
	Calcium ion binding	9.2E-11
	G-protein coupled receptor activity	1.8E-10
	Signal transducer activity	1.4E-09
	Transcription factor activity	2.8E-09
	Sugar binding	3.4E-07
Cellular component	Extracellular space	7.4E-18
	Extracellular region	9.6E-18
	Membrane	3.7E-16
	Integral to membrane	4.9E-16
	Integral to plasma membrane	2.0E-14
	External side of plasma membrane	3.4E-07

Table S2. Comparison of expression array data for *Ring1B* -KO and *Ring1A/B*-dKO ES cells

A. Average fold expression changes in *Ring1B*-KO and *Ring1A/B*-dKO (ratio of KO/control)

	Total	GO:development (*P* value)
Ring1B-KO (day 4)	1.011	1.046 (2.8×10^{-3})
Ring1A/B-dKO (day 4)	1.031	1.389 (2.4×10^{-18})
No. of probes	45,037	1006

B. Average ratios of *Ring1A/B*-dKO (day 4) to *Ring1B*-KO (day 4) for each probe

	No. of probes	dKO/KO	*P* value
Total	27,280	0.986	1.9×10^{-3}
GO:development	668	1.206	7.2×10^{-9}

Table S3. Raw data for Fig. 2B

Comparison of target binding of Ring1B in ES cells and expression changes in *Ring1B* constitutive KO ES cells

Fold enrichment	No. of genes	No. of expressed genes	No. of derepressed genes	No. of repressed genes	Mean of expression changes (KO/cont)	Mean of expression changes (log_{10})	SD	*P* value
0.0-2.5	3872	1315	674	641	1.030	0.013	0.189	1.54E-02
2.5-5.0	5103	2744	1398	1346	1.029	0.012	0.187	5.90E-04
5.0-7.5	4699	2799	1449	1350	1.033	0.014	0.187	8.34E-05
7.5-10.0	2556	1515	782	733	1.037	0.016	0.198	1.91E-03
10.0-12.5	1303	743	397	346	1.070	0.029	0.197	5.67E-05
12.5-15.0	657	368	212	156	1.127	0.052	0.214	4.21E-06
15.0-17.5	357	198	118	80	1.183	0.073	0.260	1.14E-04
17.5-20.0	172	84	51	33	1.228	0.089	0.281	4.86E-03
20.0-22.5	108	51	36	15	1.596	0.203	0.351	1.56E-04
22.5-25.0	39	12	9	3	1.250	0.097	0.199	1.34E-01
25.0+	96	43	31	12	1.463	0.165	0.398	1.02E-02

Comparison of target binding of Ring1B in ES cells and expression changes in *Ring1AB*-dKO (day 4) ES cells

Fold enrichment	No. of genes	No. of expressed genes	No. of derepressed genes	No. of repressed genes	Mean of expression changes (KO/cont)	Mean of expression changes (log_{10})	SD	*P* value
0.0-2.5	3872	1292	611	681	1.004	0.002	0.240	7.90E-01
2.5-5.0	5103	2693	1306	1387	1.012	0.005	0.235	2.55E-01
5.0-7.5	4699	2749	1354	1395	1.040	0.017	0.250	4.18E-04
7.5-10.0	2556	1510	771	739	1.097	0.040	0.276	1.68E-08
10.0-12.5	1303	753	423	330	1.217	0.085	0.313	2.04E-13
12.5-15.0	657	369	204	165	1.240	0.093	0.334	1.49E-07
15.0-17.5	357	201	120	81	1.355	0.132	0.385	2.55E-06
17.5-20.0	172	86	54	32	1.403	0.147	0.373	4.67E-04
20.0-22.5	108	53	29	24	1.662	0.221	0.491	2.07E-03
22.5-25.0	39	13	9	4	2.035	0.309	0.414	2.40E-02
25.0+	96	41	30	11	2.148	0.332	0.484	9.38E-05

Table S4. Raw data for Fig. 3C showing the average expression change by *Ring1A/B* -dKO of derepressed or repressed genes by *Oct3/4*-KO that have more than a certain value of maximum fold enrichment determined by Ring1B-ChIP

Among total genes

Fold enrichment (Ring1B-ChIP)	Number of genes	Average fold change by *Ring1A/B*-dKO (log_{10})	SD (log_{10})
0 (0-1)	4591	0.009	0.226
1 (1-2)	4552	0.010	0.226
2 (2-3)	4280	0.011	0.227
3 (3-4)	3697	0.016	0.232
4 (4-5)	2901	0.025	0.240
5 (5-6)	2191	0.031	0.242
6 (6-7)	1627	0.040	0.254
7 (7-8)	1198	0.051	0.263
8 (8-9)	856	0.061	0.285
9 (9-10)	650	0.070	0.296
10 (10-11)	454	0.101	0.316
11 (11-12)	352	0.138	0.334
12 (12-13)	294	0.149	0.354
13 (13-14)	233	0.174	0.376
14 (14-15)	188	0.182	0.376
15 (15-16)	148	0.215	0.384
16 (16-17)	122	0.201	0.380
17 (17-18)	99	0.186	0.351
18 (18-19)	82	0.218	0.360
19 (19-20)	71	0.242	0.369
20 (20-)	61	0.238	0.386

Among derepressed genes by *Oct3/4*-KO

Fold enrichment (Ring1B-ChIP)	Number of genes	Average fold change by *Ring1A/B*-dKO (log_{10})	SD (log_{10})	*P* value of *t*-test against total
0 (0-1)	129	0.247	0.375	1.23E-39
1 (1-2)	128	0.251	0.375	7.87E-40
2 (2-3)	125	0.254	0.376	6.31E-39
3 (3-4)	115	0.263	0.375	4.98E-37
4 (4-5)	92	0.283	0.391	1.15E-28
5 (5-6)	73	0.287	0.370	1.89E-25
6 (6-7)	59	0.299	0.388	3.65E-19
7 (7-8)	46	0.332	0.412	1.27E-14
8 (8-9)	36	0.384	0.428	1.90E-12
9 (9-10)	31	0.424	0.432	1.15E-11
10 (10-11)	24	0.485	0.453	3.49E-09
11 (11-12)	24	0.485	0.453	2.17E-08
12 (12-13)	21	0.490	0.480	1.28E-06
13 (13-14)	18	0.581	0.457	1.77E-07
14 (14-15)	13	0.632	0.380	4.20E-08
15 (15-16)	12	0.607	0.385	8.42E-07
16 (16-17)	10	0.556	0.335	9.11E-07
17 (17-18)	9	0.535	0.347	1.07E-05
18 (18-19)	8	0.570	0.352	4.13E-05
19 (19-20)	8	0.570	0.352	5.93E-05
20 (20+)	6	0.634	0.294	7.08E-06

Among repressed genes by *Oct3/4*-KO				
Fold enrichment (Ring1B-ChIP)	Number of genes	Average fold change by *Ring1A/B*-dKO (log_{10})	SD (log_{10})	*P* value of *t*-test against total
0 (0-1)	224	–0.119	0.331	7.83E-44
1 (1-2)	221	–0.115	0.330	3.17E-42
2 (2-3)	214	–0.116	0.334	1.30E-40
3 (3-4)	188	–0.111	0.342	1.47E-33
4 (4-5)	155	–0.081	0.344	2.30E-21
5 (5-6)	129	–0.066	0.363	9.44E-14
6 (6-7)	102	–0.034	0.352	3.79E-08
7 (7-8)	82	–0.024	0.374	7.59E-06
8 (8-9)	65	–0.041	0.388	9.19E-07
9 (9-10)	48	–0.035	0.390	1.74E-05
10 (10-11)	33	0.047	0.383	4.74E-02
11 (11-12)	26	0.101	0.397	2.45E-01
12 (12-13)	21	0.083	0.429	1.23E-01
13 (13-14)	15	0.113	0.466	3.03E-01
14 (14-15)	13	0.152	0.478	6.47E-01
15 (15-16)	9	0.236	0.474	7.92E-01
16 (16-17)	8	0.214	0.498	8.88E-01
17 (17-18)	6	0.042	0.324	1.88E-02
18 (18-19)	6	0.042	0.324	7.55E-03
19 (19-20)	4	0.128	0.244	2.03E-02
20 (20+)	3	0.060	0.247	1.69E-02